Available online at www.sciencedirect.com

ScienceDirect

Ceramics International 40 (2014) 2575–2579

CERAMICS INTERNATIONAL

www.elsevier.com/locate/ceramint

A reddish orange stoichiometric phosphor $LiEu(PO_3)_4$ for white light-emitting diodes

Zhongfei Mu[a,b], Yihua Hu[b,*], Li Chen[b], Xiaojuan Wang[b], Guifang Ju[b], Zhongfu Yang[b], Ren Chen[b]

[a]*Experimental Teaching Department, Guangdong University of Technology, Guangzhou 510006, PR China*
[b]*School of Physics and Optoelectronic Engineering, Guangdong University of Technology, Guangzhou 510006, PR China*

Received 27 August 2013; received in revised form 21 October 2013; accepted 22 October 2013
Available online 30 October 2013

Abstract

Stoichiometric phosphors $LiGd_{1-x}Eu_x(PO_3)_4$($x=0$, 0.2, 0.4, 0.6, 0.8, 1.0) were synthesized via traditional solid state reactions. The X-ray powder diffraction measurements show that all prepared samples are isostructural with $LiNd(PO_3)_4$. Eu^{3+} doped phosphors can emit intense reddish orange light under the excitation of near ultraviolet light from 370 to 410 nm. The strongest two at 591 and 613 nm can be attributed to the transitions from excited state $^5D_0$ to ground states $^7F_1$ and $^7F_2$, respectively. The typical chromaticity coordinates ($x=0.620$, $y=0.368$) of Eu^{3+} doped phosphors are in red area. The recorded absorbance spectra indicate that there is effective absorbance in the near UV region for all Eu^{3+} doped samples. Present research indicates that $LiGd_{1-x}Eu_x(PO_3)_4$ is a promising phosphor for white light-emitting diodes.

Keywords: A. $LiGd(PO_3)_4$: Eu^{3+}; B. Phosphor; C. White light-emitting diodes

1. Introduction

Phosphor-converted white light-emitting diode (LED) is an important light source of solid state illumination [1–4]. In these LEDs, tricolor phosphors are excited by near ultraviolet (NUV) InGaN-based chips to generate white light. The currently used red phosphor for NUV LEDs is Y_2O_2S: Eu^{3+} [5]. However, the efficiency of this phosphor is much weaker than blue and green phosphors. Simultaneously, it is chemically unstable. A red phosphor with high absorption in NUV spectral region and satisfying chemical stability is urgently needed for commercial applications.

Currently, alkali lanthanide phosphates were extensively investigated for their interesting optical applications [6–8]. These compounds were reported as cyclophosphates or polyphosphates with general formula $M^IM^{III}P_4O_{12}$ and can be classified into seven different structural types which usually denoted by Roman numbers from I to VII [9–11]. This nomenclature first proposed by Palkina et al. is generally accepted. $LiGd(PO_3)_4$ (LGP) is a new condensed phosphate compound in this family (type I) [12]. In Ref. [12], the structure of this novel phosphate was determined by single crystal X-ray diffraction (XRD) techniques. LGP is isostructural with $LiNd(PO_3)_4$. It crystallizes in the monoclinic space group C2/c with the unit cell parameters $a=16.386(2)$, $b=7.059(3)$, $c=9.677(2)$ Å, $\beta=126.12(1)^\circ$, $V=904.2$ Å^3 and $Z=4$. The coordination numbers (CN) of gadolinium and lithium are eight and four respectively.

Subsequently, some researchers synthesized rare earth ions doped LGP and investigated the luminescence properties of these phosphors. Zhong et al. prepared Ce^{3+} doped $MGd(PO_3)_4$(M=Li, Na, K, Cs) powder samples and investigated the luminescence properties of these phosphors under X-ray irradiation [13]. Han et al. introduced Eu^{3+} into LGP and studied the luminescence properties [14]. The results of Han and co-workers show that Eu^{3+} doped LGP can emit intense red light under the excitation of vacuum ultraviolet (VUV) light. Thus it is a promising red phosphor for mercury-free lamps and plasma display panel (PDP). However, the luminescence properties of Eu^{3+} in LGP excited with NUV lights have not been reported. Our research show Eu^{3+} doped LGP is also a promising red phosphor under the excitation of NUV light. This is very important for its applications in white light-emitting diodes.

*Corresponding author. Tel.: +86 20 39322262; fax: +86 20 39322265.
E-mail address: huyh@gdut.edu.cn (Y. Hu).

0272-8842/$ - see front matter © 2013 Elsevier Ltd and Techna Group S.r.l. All rights reserved.
http://dx.doi.org/10.1016/j.ceramint.2013.10.095

2. Experimental

All the investigated phosphors were synthesized with traditional solid state reactions. Fine powders of pure Li_2CO_3 (99.0% Sinopharm Chemical Reagent Co., Ltd., Shanghai, China), $(NH_4)_2HPO_4$ (99.0% Sinopharm Chemical Reagent Co., Ltd., Shanghai, China) Gd_2O_3 (99.99% Guangdong Research Institute of Non-ferrous Metals, Guangzhou, China), and Eu_2O_3 (Guangdong Research Institute of Non-ferrous Metals, Guangzhou, China) were used as starting materials. Firstly, raw materials were accurately weighed according to the composition of $LiGd_{1-x}Eu_x(PO_3)_4$(x=0, 0.2, 0.4, 0.6, 0.8, 1.0). To be clear, in the following depiction these samples sometimes are abbreviated as LG_5E_0P, LG_4E_1P, LG_3E_2P, LG_2E_3P, LG_1E_4P and LG_0E_5P, respectively (the numbers indicate the content of Gd^{3+} and Eu^{3+}). The weighed materials were put into an agate mortar and ground with an agate pestle in order to mix them thoroughly. Then they were heated up to 700 °C in a muffle furnace. The samples were preserved at 700 °C in air for 20 h, subsequently cooled naturally within the furnace. The cooled samples were ground again before they were measured and analyzed.

The phase identification of prepared phosphors was carried out with a Beijing MSAL-XD-2 X-ray powder diffractometer. The excitation and emission spectra of the phosphors were measured with Hitachi F-7000 fluorescence spectrophotometer. The absorption spectra of the samples were recorded with a Shimadzu UV-2450 UV–vis spectrophotometer. All the measurements were performed at room temperature. As for the details of these instruments, the reader can refer to our previous literatures [15,16].

3. Results and discussion

3.1. Phase identification

The XRD pattern of undoped LG_5E_0P was shown in Fig. 1(a). Han et al. calculated the reference XRD pattern of LGP by the program POUDRIX on the basis of the published crystal structure

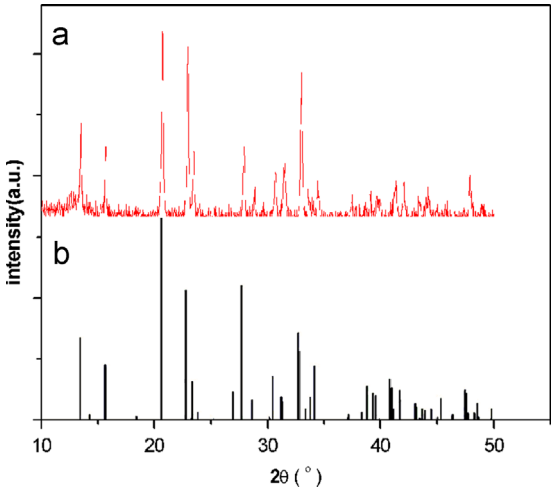

Fig. 1. The XRD pattern of LG_5E_0P (a) and calculated reference XRD pattern of LGP (b).

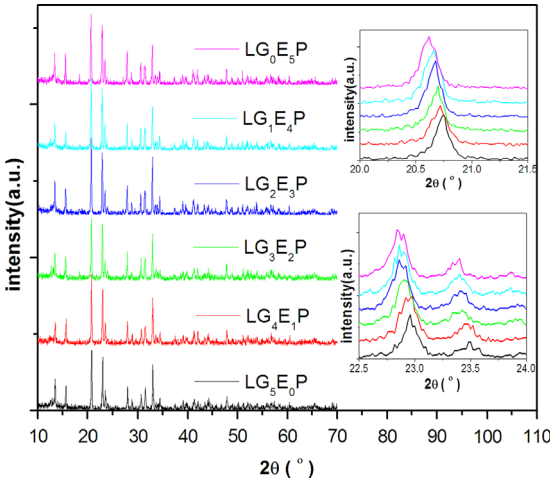

Fig. 2. The XRD patterns of all prepared samples (the insets show the magnified part in the main graph).

[14]. In this work, the XRD pattern of LGP obtained by them was cited as a reference in Fig. 1(b). From Fig. 1, it can be clearly observed that the XRD pattern of LG_5E_0P is consistent with the calculated one. This indicates that expected phase LGP has been obtained.

Fig. 2 shows the XRD patterns of samples with the different Eu^{3+} content. All the patterns are same at first sight. However, if we magnify these patterns locally it can be seen that there is slight difference in the position of diffraction peaks. The insets show the magnified part of the XRD patterns. It is clearly observed that from LG_5E_0P to LG_0E_5P, in the process of the increment of Eu^{3+} content, the main diffraction peaks of samples gradually move to lower angles. According to Bragg's equation $2d\sin\theta=\lambda$ (here λ is the wavelength of employed X-ray, λ=0.15406 nm, θ and d are diffraction angle and interplanar distance of corresponding diffraction peak, respectively), the shifting to lower angles of the peaks indicates that the interplanar distance of samples is increasing. According to the radii of involved ions (R (P_4^{5+})=0.017 nm, R (Li_4^{+})=0.059 nm, R (Gd_8^{3+})=0.1053 nm, R (Eu_8^{3+})=0.1066 nm (the subscript here denotes the CN of the cation) [17] and the ratio of starting materials, it is expected that Eu^{3+} replace Gd^{3+}. There is no obvious impurity peaks in the XRD patterns of Eu^{3+} doped samples in Fig. 2. This indicates all the Eu^{3+} come into Gd^{3+} sites according to our anticipation. The ionic radius of Eu^{3+} is slightly bigger than Gd^{3+}. This is just the reason for the increasing of interplanar distance of samples.

3.2. Photoluminescence properties of $LiGd_{1-x}Eu_x(PO_3)_4$

Fig. 3 shows the emission spectra under 394 nm excitation. From Fig. 3, it is observed that undoped LG_5E_0P does not emit any light. However when Eu^{3+} is introduced into host lattice (LG_4E_1P), some emission lines appear in the spectral range from 500 to 750 nm. The strongest two at 591 and 613 nm can be attributed to the transitions from excited state $^5D_0$ to ground states $^7F_1$ and $^7F_2$, respectively. The rest emission lines can also be observed at 700 nm ($^5D_0 \rightarrow {}^7F_4$), 651 nm ($^5D_0 \rightarrow {}^7F_3$),

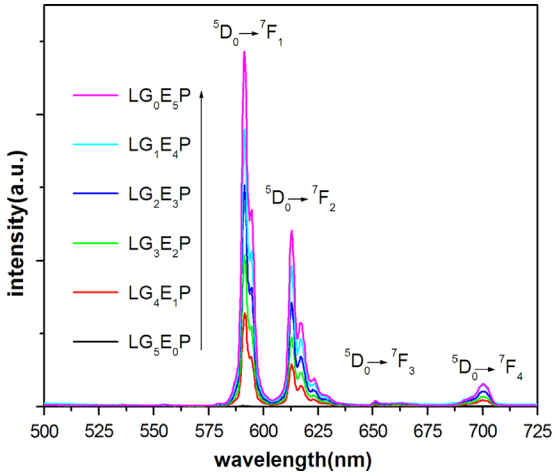

Fig. 3. The emission spectra of all prepared samples excited with 394 nm.

but they are much weaker than the former two ones. The predominance of the emission lines from $^5D_0$ to $^7F_1$ and $^7F_2$ might be attributed to the coupling of the vibration energy of the host lattice and the gaps between the higher energy levels ($^5D_1$ or $^5D_2$) and the $^5D_0$ level of Eu^{3+} [18]. Emission from higher levels is quenched by the multi-phonon relaxation.

As is well-known, if Eu^{3+} occupies a site in the crystal lattice with inversion symmetry, the magnetic dipole (MD) transition $^5D_0 \rightarrow {}^7F_1$ of Eu^{3+} dominates; if there is no inversion symmetry at the site of Eu^{3+}, the main emission is the electric dipole (ED) transition $^5D_0 \rightarrow {}^7F_2$ [19]. From Fig. 3, the orange emission from transition $^5D_0 \rightarrow {}^7F_1$ is dominant and integrating intensity ratio of $^5D_0 \rightarrow {}^7F_1$ (from 580 to 605 nm) / $^5D_0 \rightarrow {}^7F_2$ (from 605 to 635 nm) is about 1.56 [20]. This ratio does not change with the increment of the doping concentration of Eu^{3+}. This indicates that Eu^{3+} occupies a site in the crystal lattice with inversion symmetry. However, the GdO_8 dodecahedra are considerably distorted in LGP [12]. Thus, the inversion symmetry of Eu^{3+} site is incomplete. Furthermore, the substitution of Eu^{3+} for Gd^{3+} could result in slight distortion of the crystal lattice. All these factors make the ED transition $^5D_0 \rightarrow {}^7F_2$ presents a rather intensity.

From Fig. 3, it can also be observed that with the increment of Eu^{3+} content, both emission peaks increases monotonically. LG_0E_5P has the strongest emission. Concentration quenching of Eu^{3+} luminescence does not happen even if the doping concentration of Eu^{3+} was enhanced to 100% of Gd^{3+}, i.e. Eu^{3+} replace Gd^{3+} totally. The electric multipole interactions between Eu^{3+} ions are weak due to the weak oscillator strength of $^7F_0 \rightarrow {}^5D_0$ [21], so only exchange interactions are important. However, the critical distance for exchange interactions between Eu^{3+} ions is about 0.5 nm [22], while the minimum Gd−Gd distance in LGP is about 0.5617 nm [12]. We suppose that in the case of $LiEu(PO_4)_3$ it is similar. Thus, energy migration over Eu^{3+} sublattice cannot take place effectively.

The Commission Internationale de L'Eclairage (CIE) chromaticity coordinates of Eu^{3+} doped phosphors excited at 394 nm were calculated with the data of emission spectra. Phosphors with different doping concentration of Eu^{3+} own the same coordinates for their same spectral shape. Fig. 4

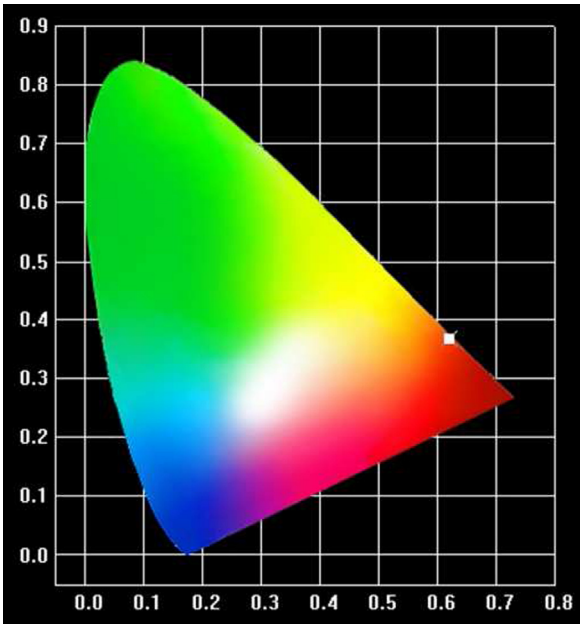

Fig. 4. The position of chromaticity coordinates ($x=0.620$, $y=0.368$) of LG_0E_5P.

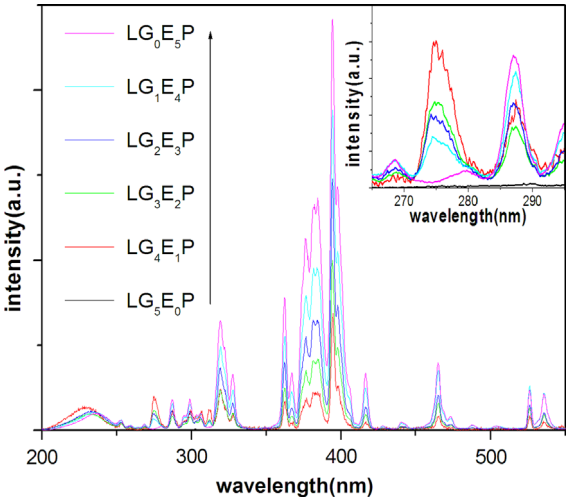

Fig. 5. The excitation spectra of all prepared samples monitoring the emission at 591 nm (the inset shows the magnified part surrounded by a rectangle in the main graph).

shows the position of typical chromaticity coordinates ($x=0.620$, $y=0.368$) of LG_0E_5P with a white square. It is in the red area.

Fig. 5 shows the excitation spectra of samples monitoring the emission at 591 nm. It is observed that all the excitation spectra are composed of one broad band from 200 to 250 nm and a group of excitation lines in UV and visible region. In most of hosts, the charge transfer (CT) band of Eu^{3+} locates between 30,000 and 45,000 cm^{-1}(i.e. between 222 and 333 nm) [23]. Thus the broad band from 200 to 250 nm can be attributed to the CT band of Eu^{3+}. The excitation lines can be attributed to the intra-configurational 4f−4f transitions of Eu^{3+} in the host lattice: $^7F_0 \rightarrow {}^5F_J$ (287, 299 nm), $^7F_0 \rightarrow {}^5H_6$

(319 nm), $^7F_0 \rightarrow {}^5H_3$ (328 nm), $^7F_0 \rightarrow {}^5D_4$ (362 nm), $^7F_0 \rightarrow {}^5L_8$ (367 nm), $^7F_0 \rightarrow {}^5G_3$ (376 nm), $^7F_0 \rightarrow {}^5L_7$ (385 nm), $^7F_0 \rightarrow {}^5L_6$ (394 nm), $^7F_0 \rightarrow {}^5D_3$ (417 nm), $^7F_0 \rightarrow {}^5D_2$ (465 nm), $^7F_0 \rightarrow {}^5D_1$ (526 nm) and $^7F_1 \rightarrow {}^5D_1$ (536 nm), respectively [24]. At room temperature, the $^7F_1$ level is thermally populated due to the small energy gap of $^7F_1$ and $^7F_0$ ($\sim 370\ cm^{-1}$), so the transition of $^7F_1$-$^5D_1$ was observed at 536 nm. Excitation intensity of these excitation lines is much stronger than CT band. Most of the excitation lines are broadened and some of them overlap together. The splitting of energy levels due to the crystal field effect is responsible for the broadening of the excitation lines. The line broadening might also occur because some Eu^{3+} occupy different crystallographic sites, thus, emitting at different wavelength.

Particularly, some broadened excitation lines overlap together and form a strong excitation band from 370 to 410 nm with a full width at half maximum(FWHM) of 18 nm. The perfect matching of this excitation band with the emission wavelength of NUV InGaN-based LED chips makes these phosphors be used in white LEDs conveniently.

From Fig. 5, it is observed that excitation intensity changes with the increment of doping concentration of Eu^{3+}. However, the shape and position of excitation peaks or band do not change except for the slight alternation in the region from 270 to 280 nm (which can be observed obviously in the inset of Fig. 5). With the increment of the Eu^{3+} content, excitation intensity in this region firstly increases, reaches a maximum, then decreases. The subtle change about the excitation line at 275 nm can be attributed to the transition from ground state $^8S_{7/2}$ to excited state $^6I_{7/2}$ of Gd^{3+} [25–28]. It indicates that weak energy transfer from Gd^{3+} to Eu^{3+} happens when they coexist in the host.

We also recorded the excitation spectra of samples monitoring the emission at 613 nm. The situation is basically same to Fig. 5 except for different excitation intensity.

The absorption spectra of all the samples were recorded and listed in Fig. 6. It can be observed that there is effective absorbance in the near UV region for all Eu^{3+} doped samples. The changing trend of the absorbance with the alternation of

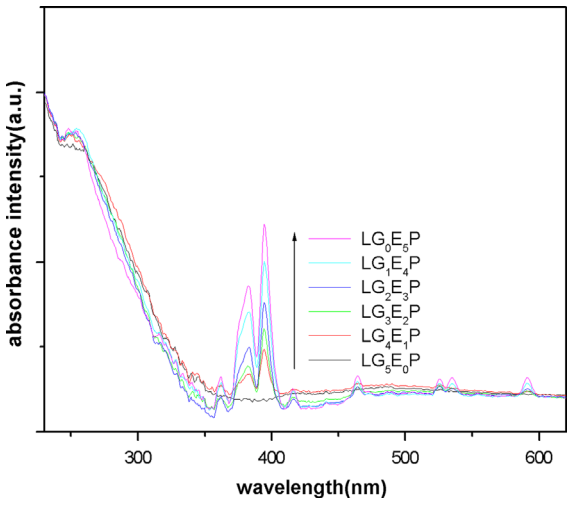

Fig. 6. The absorption spectra of all prepared samples.

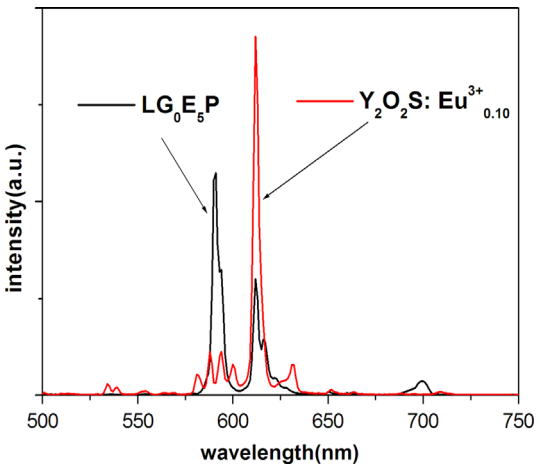

Fig. 7. The comparison of PL spectra of LG_0E_5P and Y_2O_2S: $Eu^{3+}_{0.10}$.

Eu^{3+} content is coincident with the one of the excitation intensity. The fundamental absorption edge of LGP locates at $\sim$350 nm (Fig. 6). However, there is no obvious excitation in the spectral region below 350 nm (Fig. 5). This indicates that excitation energy absorbed by the host cannot be transferred to Eu^{3+} effectively. In LGP, Gd^{3+} are in the center of GdO_8 dodecahedra and Eu^{3+} mainly replace Gd^{3+}. Gd^{3+} and Eu^{3+} are effectively isolated. This results in the absence of effective energy transfer from the host to doped Eu^{3+}.

PL spectra of LG_0E_5P and commercially obtained Y_2O_2S: $Eu^{3+}_{0.10}$ excited with 394 nm UV light are exhibited in Fig. 7. It is observed that both phosphors have emission in reddish orange spectral region. However, the strongest emission peaks locate at different positions, 591 nm for the former while 613 nm for the latter. The peak intensity of the former is comparable with the latter. Integrated reddish orange emission intensity (from 580 to 640 nm) of LG_0E_5P is about 88% of the one of Y_2O_2S: $Eu^{3+}_{0.10}$. This indicates that $LiEu(PO_3)_4$ is a promising reddish orange phosphor for white LEDs.

4. Conclusions

A series of phosphors with the composition $LiGd_{1-x}Eu_x(PO_3)_4$(x=0, 0.2, 0.4, 0.6, 0.8, 1.0) were synthesized by solid state reaction. The structures and photoluminescence properties of these phosphors were investigated at room temperature. All prepared samples are proved to be isostructural with $LiNd(PO_3)_4$ by the XRD measurements. Eu^{3+} doped phosphors can be effectively excited by NUV light from 370 to 410 nm and emit intense reddish orange light. The orange emission from transition $^5D_0 \rightarrow {}^7F_1$ is dominant and integrating intensity ratio of $^5D_0 \rightarrow {}^7F_1/{}^5D_0 \rightarrow {}^7F_2$ is about 1.56. The typical chromaticity coordinates (x=0.620, y=0.368) of Eu^{3+} luminescence are in red area. The absence of concentration quenching of Eu^{3+} emission was observed in $LiGd_{1-x}Eu_x(PO_3)_4$. Recorded absorbance spectra indicate that there is effective absorbance in the near UV region for all Eu^{3+} doped samples. The fundamental absorption edge of LGP locates at $\sim$350 nm. The perfect match of the excitation band of Eu^{3+} with the

emission wavelength of current NUV LEDs indicates that $LiGd_{1-x}Eu_x(PO_3)_4$ is a promising phosphor for white LED.

Acknowledgement

This research was supported by the National Natural Science Foundations of China (Grant Nos. 21271049). We are grateful to Mr. Z.D. Hao for helpful discussions.

References

[1] R. Mueller-Mach, G.O. Mueller, M.R. Krames, T. Trottier, High-power phosphor-converted light-emitting diodes based on III-nitrides, IEEE J. Sel. Top. Quantum Electron. 8 (2002) 339–345.
[2] J.H. Yum, S.Y. Seo, S. Lee, Y.E. Sung, $Y_3Al_5O_{12}$: $Ce_{0.05}$ phosphor coatings on gallium nitride for white light emitting diodes, J. Electrochem. Soc. 150 (2003) H47–H52.
[3] J.S. Kim, P.E. Jeon, Y.H. Park, J.C. Choi, H.L. Park, G.C. Kim, T. W. Kim, White-light generation through ultraviolet-emitting diode and white-emitting phosphor, Appl. Phys. Lett. 85 (2004) 3696–3698.
[4] J.K. Park, C.H. Kim, S.H. Park, H.D. Park, S.Y. Choi, Application of strontium silicate yellow phosphor for white light-emitting diodes, Appl. Phys. Lett. 84 (2004) 1647–1649.
[5] S. Neeraj, N. Kijima, A.K. Cheetham, Novel red phosphors for solid-state lighting: the system $NaM(WO_4)_{2-x}$ $(MoO_4)_x$: Eu^{3+} (M=Gd, Y, Bi), Chem. Phys. Lett. 387 (2004) 2–6.
[6] I. Parreu, R. Sole, Jna. Gavalda, J. Massons, F. Diaz, M. Aguilo, Crystallization region, crystal growth, and phase transitions of KNd $(PO_3)_4$, Chem. Mater. 15 (2003) 5059–5064.
[7] K. Horchani, J.C. Gacon, M. Ferid, M. Trabelsi-Ayedi, O. Krachni, G. K. Liu, Energy levels of Pr^{3+} in $CsPrP_4O_{12}$ and $RbPrP_4O_{12}$ cyclotetraphosphates, Opt. Mater. 24 (2003) 169–174.
[8] M. Saito, T. Honma, Y. Benino, T. Fujiwara, T. Komatsu, Formation of nonlinear optical $KSm(PO_3)_4$ crystals in phosphate glasses by YAG laser irradiation, Solid State Sci. 6 (2004) 1013–1018.
[9] H. Ettis, H. Naili, T. Mhiri, Synthesis and crystal structure of a new potassium-gadolinium cyclotetraphosphate, $KGdP_4O_{12}$, Cryst. Growth Des. 3 (2003) 599–602.
[10] W. Rekik, H. Naili, T. Mhiri, Potassium gadolinium polyphosphate, KGd $(PO_3)_4$, Acta Crystallogr. Sect. C: Cryst. Struct. Commun. 60 (2004) I50–I52.
[11] H. Naili, T. Mhiri, Caesium gadolinium polyphosphate, $CsGd(PO_3)_4$, Acta Crystallogr. Sect. E: Struct. Rep. Online. e61 (2005) I204–I207.
[12] H. Ettis, H. Naili, T. Mhiri, The crystal structure, thermal behaviour and ionic conductivity of a novel lithium gadolinium polyphosphate LiGd $(PO_3)_4$, J. Solid State Chem. 179 (2006) 3107–3113.
[13] J.P. Zhong, H.B. Liang, Q. Su, J.Y. Zhou, I.V. Khodyuk, P. Dorenbos, Radioluminescence properties of Ce^{3+}-activated $MGd(PO_3)_4$ (M=Li, Na, K, Cs), Opt. Mater. 32 (2009) 378–381.
[14] B. Han, H.B. Liang, H.Y. Ni, Q. Su, G.T. Yang, J.Y. Shi, G.B. Zhang, Intense red light emission of Eu^{3+}-doped $LiGd(PO_3)_4$ for mercury-free lamps and plasma display panels application, Opt. Express 17 (2009) 7138–7144.
[15] Z.F. Mu, Y.H. Hu, L. Chen, X.J. Wang, Enhanced red emission in Sr_2CeO_4: Eu^{3+} by charge compensation, J. Electrochem. Soc. 158 (2011) J287–J290.
[16] Z.F. Mu, Y.H. Hu, L. Chen, X.J. Wang, Enhanced luminescence of Dy^{3+} in $Y_3Al_5O_{12}$ by Bi^{3+} co-doping, J. Lumin. 131 (2011) 1687–1691.
[17] R.D. Shannon, Revised effective ionic radii and systematic studies of interatomic distances in halides and chalcogenides, Acta Crystallogr. Sect. A: Found. Crystallogr 32 (1976) 751–767.
[18] M. Yu, J. Lin, Z. Wang, J. Fu, S. Wang, H.J. Zhang, Y.C. Han, Fabrication, patterning, and optical properties of nanocrystalline YVO_4: A (A=Eu^{3+}, Dy^{3+}, Sm^{3+}, Er^{3+}) phosphor films via sol−gel soft lithography, Chem. Mater. 14 (2002) 2224–2231.
[19] M. Gaft, G. Panczer, R. Reisfeld, I. Shinno, B. Champagnon, G. Boulon, Laser-induced Eu^{3+} luminescence in zircon $ZrSiO_4$, J. Lumin. 87 (2000) 1032–1035.
[20] A. Katelnikovas, J. Plewa, S. Sakirzanovas, D. Dutczak, D. Enseling, F. Baur, H. Winkler, A. Kareiva, T. Jüstel, Synthesis and optical properties of $Li_3Ba_2La_3(MoO_4)_8$: Eu^{3+} powders and ceramics for pcLEDs, J. Mater. Chem. 22 (2012) 22126–22134.
[21] W.T. Carnall, P.R. Fields, K. Rajnak, Spectral intensities of the trivalent lanthanides and actinides in solution. II. Pm^{3+}, Sm^{3+}, Eu^{3+}, Gd^{3+}, Tb^{3+}, Dy^{3+} and Ho^{3+}, J. Chem. Phys. 49 (1968) 4412–4423.
[22] G. Blasse, Luminescence of inorganic solids: from isolated centers to concentrated systems, Prog. Solid State Chem. 18 (1988) 79–171.
[23] G. Blasse, Reminiscencies of a quenched luminescence investigatory, J. Lumin 100 (2002) 65–67.
[24] Y. Li, Y. Chang, Y. Lin, Y. Chang, Y. Lin, Synthesis and luminescent properties of Ln^{3+} (Eu^{3+}, Sm^{3+}, Dy^{3+})-doped lanthanum aluminum germinate $LaAlGe_2O_7$ phosphors, J. Alloys Compd. 439 (2007) 367–375.
[25] A.J. de Vries, M.F. Hazenkamp, G. Blasse, On the Gd^{3+} luminescence and energy migration in $Li(Y,Gd)F_4$-Tb^{3+}, J. Lumin 42 (1988) 275–282.
[26] H. Kondo, T. Hirai, S. Hashimoto, Energy transfer through Gd^{3+} sublattice in the fluoride phosphors, J. Lumin. 94–95 (2001) 311–315.
[27] A. Kumar, D.K. Rai, S.B. Rai, Luminescence of Gd^{3+} ions doped in oxyfluoroborate glass, Solid State Commun. 117 (2001) 387–392.
[28] Y.C. Li, Y.S. Chang, Y.C. Lai, Y.J. Lin, C.H. Laing, Y.H. Chang, Luminescence and energy transfer properties of Gd^{3+} and Tb^{3+} in $LaAlGe_2O_7$, Mater. Sci. Eng. B 146 (2008) 225–230.